symmetry

MDPI

Article

The Entanglement Generation in $\mathcal{PT}$-Symmetric Optical Quadrimer System

Joanna K. Kalaga [1,2]

[1] Quantum Optics and Engineering Division, Institute of Physics, University of Zielona Góra, Prof. Z. Szafrana 4a, 65-516 Zielona Góra, Poland; j.kalaga@if.uz.zgora.pl

[2] Joint Laboratory of Optics of Palacký University and Institute of Physics of CAS, Faculty of Science, Palacký University, 17. listopadu 12, 771 46 Olomouc, Czech Republic

Received: 12 July 2019; Accepted: 29 August 2019; Published: 3 September 2019

Abstract: We discuss a model consisting of four single-mode cavities with gain and loss energy in the first and last modes. The cavities are coupled to each other by linear interaction and form a chain. Such a system is described by a non-Hermitian Hamiltonian which, under some conditions, becomes $\mathcal{PT}$-symmetric. We identify the phase-transition point and study the possibility of generation bipartite entanglement (entanglement between all pairs of cavities) in the system.

Keywords: $\mathcal{PT}$-symmetry; entanglement; negativity

1. Introduction

One of the main principles of quantum mechanics is the assumption that the Hamiltonian describing a quantum system must be Hermitian. In consequence, all of Hamiltonian's eigenvalues are real. In 1998, Bender and Boettcher [1] showed that the Hermiticity of a Hamiltonian ($\hat{H} = \hat{H}^{\dagger}$) is not the only condition to obtain its real eigenvalues. When non-Hermitian Hamiltonian has $\mathcal{PT}$ symmetry, its eigenvalues are real. $\mathcal{PT}$ symmetry means that the Hamiltonian satisfies commutation relations $\left[\hat{H}, \hat{P}\hat{T}\right] = 0$, where $\hat{P}$ is a linear parity operator which changes the sign of the momentum operator and the position operator; whereas $\hat{T}$ is the antilinear time reversal operator.

The first of the studied $\mathcal{PT}$-symmetric Hamiltonians with a real spectrum was that described by the equation $\hat{H} = \hat{p}^2 + i\hat{x}^3$ [1–3]. The most commonly discussed quantum mechanical systems with $\mathcal{PT}$ symmetry are those described by Hamiltonians including a complex potential. When the imaginary part has a plus sign, the system obtains energy from the environment; whereas the minus sign means that the system gives energy into the environment. When the system satisfies $\mathcal{PT}$ symmetry, the loss and gain must be balanced. For optical $\mathcal{PT}$-symmetric systems, the refractive index n can play a role of the potential energy V [4]. Quantum optical systems should also exhibit such balance between the gain and loss of energy to satisfy $\mathcal{PT}$ symmetry condition. For such a case, the refractive index obeys the symmetry relation $n(x) = n^*(-x)$.

In recent years, the different kinds of $\mathcal{PT}$-symmetric systems have been considered. For instance, there has been the pair of coupled LC circuits [5], optical lattice [6,7], optomechanical system [8], optical waveguides [9], quantum-dot [10], and others. The $\mathcal{PT}$-symmetric systems can exhibit numerous interesting phenomena such as invisibility [11], chaos induced by the $\mathcal{PT}$ symmetry breaking [12], and many others.

For the $\mathcal{PT}$-symmetric system, we can observe a phase-transition point which is the point where the system loses its $\mathcal{PT}$-symmetric properties. If the system is in the $\mathcal{PT}$-symmetric phase, all eigenvalues of Hamiltonian are real. When the system is in $\mathcal{PT}$ symmetry broken phase, it has complex eigenvalue spectra. Such a transition point from the unbroken $\mathcal{PT}$-symmetric phase to the $\mathcal{PT}$ symmetry broken phase is called exceptional point [13–15]. In general, this singular point

occurs when eigenvalues and corresponding eigenvectors of the system depend on some parameters. When those parameters reach a critical value, then eigenvalues of the system coalesce and the spectrum becomes complex. If two eigenvalues coalescence, we have second-order exceptional points. During recent years, various type of singularities and their features have been studied [16–22]. The $\mathcal{PT}$-symmetric systems exhibit many interesting phenomena related to the presence of an exceptional point. For instance, enhancing spontaneous emission [23], unidirectional invisibility in fiber networks [24], and loss-induced lasing [25].

In this paper, we concentrate on the entangled states generation in the $\mathcal{PT}$-symmetric quadrimer system. In particular, we are interested in producing bipartite entangled states, and the influence of gain and loss rate on producing such states. The generation of entanglement in various quantum systems is one of the fundamental areas of interest in quantum information theory. Entanglement can be observed in various physical systems such as Bose–Einstein condensates [26,27], cavity QED [28], quantum dots [29,30], trapped ions [31], and many others [32–37]. The research related to the production of entanglement in open systems is of particular importance. For such a system, a crucial role is played by the decoherence processes, which are the consequence of the interaction of the system with the environment. One should realize that the entanglement is very sensitive to the noise processes. The interaction with the environment leads to losses of coherence, and, in consequence, destroys entanglement. Very interesting is sudden death and the rebirth of entanglement observed in various systems interacting with the environment [38–41].

The paper is organized as follows. In Section 2, we describe the $\mathcal{PT}$-symmetric system. In particular, we derive the formulas determining the location of the exceptional point, the point where the system loses its $\mathcal{PT}$ symmetry, then, the eigenvalues of Hamiltonian become complex. For the different values of gain/loss rate, we analyze the possibility of generation entanglement state in Section 3. We show how the gain/loss rate influences the entanglement production process.

2. The Model

The considered system is composed of four identical single-mode cavities of the resonance frequency ω. The first cavity is passive (it loses the energy), the second and third ones are neutral (no losses and no gain of the energy), and the last one is active (it gains the energy). All cavities are coupled mutually by linear interaction and form a chain (see Figure 1). Such a system can be described by the following Hamiltonian:

$$\begin{aligned} \hat{H} &= (\omega - i\gamma)\,\hat{a}_1^\dagger \hat{a}_1 + \omega \hat{a}_2^\dagger \hat{a}_2 + \omega \hat{a}_3^\dagger \hat{a}_3 + (\omega + i\gamma)\,\hat{a}_4^\dagger \hat{a}_4 \\ &\quad + \beta\left(\hat{a}_1^\dagger \hat{a}_2 + \hat{a}_2^\dagger \hat{a}_1 + \hat{a}_2^\dagger \hat{a}_3 + \hat{a}_3^\dagger \hat{a}_2 + \hat{a}_3^\dagger \hat{a}_4 + \hat{a}_4^\dagger \hat{a}_3\right), \end{aligned} \tag{1}$$

where $\hat{a}_i$ and $\hat{a}_i^\dagger$ are bosonic annihilation and creation operators, respectively, whereas the indices $1, 2, 3, 4$ label four subsystems. The parameter β describes the strength of linear interaction between two nearest cavities and γ denotes the strength of decay or the gain of cavities. We assume here that $\hbar = 1$ and the parameters ω, γ, and β are real.

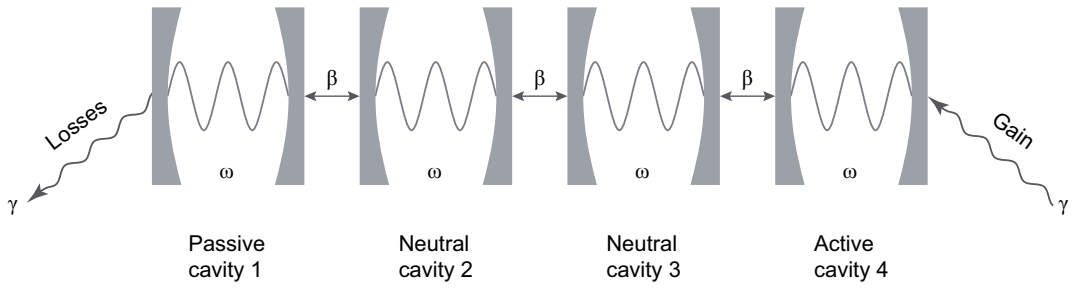

Figure 1. Scheme of the model.

The Hamiltonian defined in Equation (1) is non-Hermitian, but for some situations it becomes $\mathcal{PT}$-symmetric and its eigenvalues are real. To find the $\mathcal{PT}$ phase transition point, we write the Hamiltonian $\hat{H}$ in this form:

$$\hat{H} = \begin{bmatrix} \hat{a}_1^\dagger & \hat{a}_2^\dagger & \hat{a}_3^\dagger & \hat{a}_4^\dagger \end{bmatrix} \mathcal{H} \begin{bmatrix} \hat{a}_1 \\ \hat{a}_2 \\ \hat{a}_3 \\ \hat{a}_4 \end{bmatrix}, \tag{2}$$

where

$$\mathcal{H} = \begin{bmatrix} \omega - i\gamma & \beta & 0 & 0 \\ \beta & \omega & \beta & 0 \\ 0 & \beta & \omega & \beta \\ 0 & 0 & \beta & \omega + i\gamma \end{bmatrix}. \tag{3}$$

Next, we can calculate the eigenvalues of the Hamiltonian $\mathcal{H}$, and they are

$$\begin{aligned} E_1 &= \tfrac{1}{2}\left(2\omega - \sqrt{2}\sqrt{3\beta^2 - \sqrt{5\beta^4 - 2\beta^2\gamma^2 + \gamma^4} - \gamma^2}\right), \\ E_2 &= \tfrac{1}{2}\left(2\omega + \sqrt{2}\sqrt{3\beta^2 - \sqrt{5\beta^4 - 2\beta^2\gamma^2 + \gamma^4} - \gamma^2}\right), \\ E_3 &= \tfrac{1}{2}\left(2\omega - \sqrt{2}\sqrt{3\beta^2 + \sqrt{5\beta^4 - 2\beta^2\gamma^2 + \gamma^4} - \gamma^2}\right), \\ E_4 &= \tfrac{1}{2}\left(2\omega + \sqrt{2}\sqrt{3\beta^2 + \sqrt{5\beta^4 - 2\beta^2\gamma^2 + \gamma^4} - \gamma^2}\right). \end{aligned} \tag{4}$$

We see that all eigenvalues depend on the frequency ω, the strength of coupling β, and the gain and loss rate γ. The eigenvalues are real when two relations are satisfied simultaneously: $\left(3\beta^2 - \sqrt{5\beta^4 - 2\beta^2\gamma^2 + \gamma^4} - \gamma^2\right) \geq 0$ and $\left(3\beta^2 + \sqrt{5\beta^4 - 2\beta^2\gamma^2 + \gamma^4} - \gamma^2\right) \geq 0$.

In Figure 2a,b the real and imaginary parts of E_i are presented, respectively. We see there that the phase-transition point is localized when $\gamma = \beta$. If the gain/loss rate γ is smaller than the coupling parameter β, the spectrum is real and the system is in the $\mathcal{PT}$-symmetric phase. As the parameter γ exceeds β, the system passes into the broken $\mathcal{PT}$-symmetric phase, and the eigenvalues become complex. Observed here, the phase-transition point is the second-order exceptional point at which the two eigenvalues coalesce.

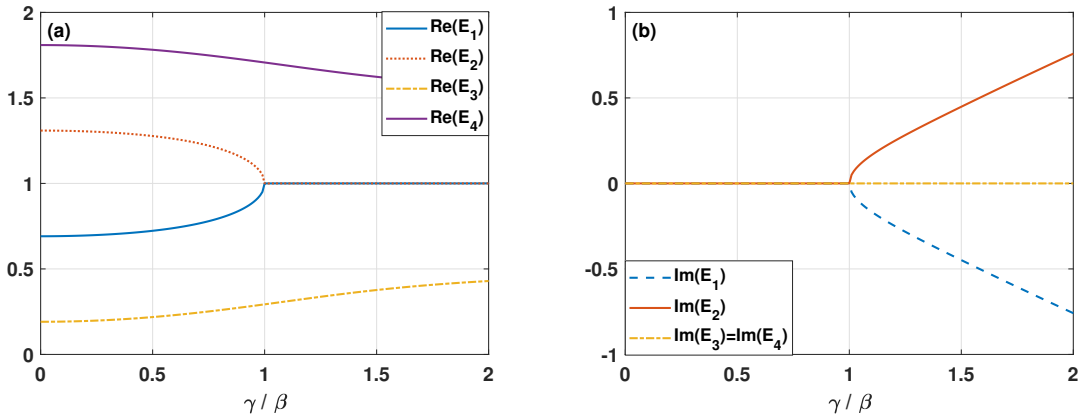

Figure 2. The values of (**a**) the real part of E_i and (**b**) the imaginary part of E_i, as a function of ratio γ/β. All parameters are scaled in ω units and $\beta = \omega/2$.

To study the system's dynamics, we analyze the time evolution of the density matrix $\hat{\rho}$. We can note that $\mathcal{PT}$-symmetric system is an open system which exchanges energy with the environment. The energy is gained and lost by the system. The evolution of such a system is determined by a master equation for the operator $\hat{\rho}$

$$\frac{d}{dt}\hat{\rho} = -i\left[\hat{H}_0, \hat{\rho}\right] + \mathcal{L}\hat{\rho}, \tag{5}$$

where

$$\hat{H}_0 = \omega\left(\hat{a}_1^\dagger\hat{a}_1 + \hat{a}_2^\dagger\hat{a}_2 + \hat{a}_3^\dagger\hat{a}_3 + \hat{a}_4^\dagger\hat{a}_4\right) + \beta\left(\hat{a}_1^\dagger\hat{a}_2 + \hat{a}_2^\dagger\hat{a}_1 + \hat{a}_2^\dagger\hat{a}_3 + \hat{a}_3^\dagger\hat{a}_2 + \hat{a}_3^\dagger\hat{a}_4 + \hat{a}_4^\dagger\hat{a}_3\right), \tag{6}$$

and $\mathcal{L}$ is the Liouvillian superoperator, which in our case it takes the form:

$$\mathcal{L}\hat{\rho} = \gamma\left(2\hat{a}_1\hat{\rho}\hat{a}_1^\dagger - \hat{a}_1^\dagger\hat{a}_1\hat{\rho} - \hat{\rho}\hat{a}_1^\dagger\hat{a}_1\right) + \gamma\left(2\hat{a}_4^\dagger\hat{\rho}\hat{a}_4 - \hat{a}_4\hat{a}_4^\dagger\hat{\rho} - \hat{\rho}\hat{a}_4\hat{a}_4^\dagger\right). \tag{7}$$

In Equation (7), the first term describes the loss and the second term is related to the gain of energy.

In further considerations, we assume that initially only one of the four cavities is in the one-photon state $|1\rangle$, and the other three are in vacuum state $|0\rangle$. Therefore, we will discuss here four cases:

- $\hat{\rho}(t=0) = |1000\rangle\langle 1000|$;
- $\hat{\rho}(t=0) = |0010\rangle\langle 0010|$;
- $\hat{\rho}(t=0) = |0100\rangle\langle 0100|$;
- $\hat{\rho}(t=0) = |0001\rangle\langle 0001|$,

where $|ijkl\rangle = |i\rangle_1 \otimes |j\rangle_2 \otimes |k\rangle_3 \otimes |l\rangle_4$ are the four-mode states. For the first of them, only the passive cavity is in the one-photon state at the initial time, then, the density matrix describing the system can be written as $|1000\rangle\langle 1000|$. The next two cases analyzed correspond to the situation when one of the neutral cavities is in the one-photon state. Finally, for the last situation discussed here, the system starts evolution from the state $|0001\rangle\langle 0001|$. For such a case, only the active cavity is in the one-photon state at the initial time.

3. The Entanglement Generation

In further considerations, we discuss the generation of two-mode entangled states. For the analysis of the degree of bipartite entanglement between two cavities, we apply the entanglement measure which is based on the positive partial transposition criterion, the *bipartite negativity*. It was defined in [42,43] as

$$N_{ij}(\rho_{ij}) = \frac{1}{2}\sum_i |\lambda_n| - \lambda_n, \tag{8}$$

where $\rho_{ij} = Tr_{k,l}\left(\rho_{ijkl}\right)$ is the two-mode density matrix, λ_n is n-th eigenvalue of the matrix $\rho_{ij}^{T_i}$, and $\rho_{ij}^{T_i}$ describes the partial transposition (with respect to the i-th mode) of the two-mode density matrix ρ_{ij}.

In our consideration, we analyze only maximal values of the bipartite negativity N_{0110} defined in the space of four two-mode states: $|0\rangle|0\rangle$; $|0\rangle|1\rangle$; $|1\rangle|0\rangle$; and $|1\rangle|1\rangle$. Therefore, to quantify the bipartite entanglement, we chose the negativity because this quantity can clearly differentiate between entangled and unentangled states when it is applied to two-qubit or qubit—qutrit systems. The negativity takes values between 0 for separable states and 1 for maximally entangled ones. To find values of N_{0110}, we generate the time evolution of the density matrix for the whole system, next, we find the reduced density matrix ρ_{ij} and calculate negativities for the subsystems spanned in the four states. We note that for the system described by $\mathcal{PT}$-symmetric Hamiltonian, its evolution is nonunitary. Therefore, we should normalize the density matrix during the all evolution-time, and then, calculate the negativity with the application of such normalized density matrix ρ_{ijkl}.

As it was mentioned before, we study the possibility of generation of the two-mode entangled state for four cases related to the four initial states (see Figure 3).

First, we consider the situation when the first cavity (passive cavity) is excited, and the initial state is $\hat{\rho}(t=0) = |1000\rangle\langle 1000|$. In Figure 3a, we show the dependence of the maximal values of negativities N_{0110} on γ/β. One can see that only entanglement between modes 1-2 can be produced for all situations considered here. What is relevant is that the degree of entanglement appearing in the system strongly depends on the value of the gain/loss parameter. With the increased value of parameter γ, we can observe decreasing entanglement in all pairs modes. For example, when $\gamma = 0.99\beta$, the maximal value of N_{12} becomes closed to 0.14. For small values of γ/β, the entanglement between all pairs of cavities is generated. Whereas for large values of γ/β, the entanglement corresponding to pairs of cavities 1-3, 1-4, 2-3, 2-4, 3-4 is not produced.

Next, we check the system's ability to produce entanglement when the evolution of our system starts from the state $\hat{\rho}(t=0) = |0100\rangle\langle 0100|$. For such a case, the excitation initially appears in the second cavity (the cavity without loss and gain). In Figure 3b, we see that analogously as in the previous case, the entanglement between all cavities is generated only for small values of γ/β and the strength of maximal possible bipartite entanglement depends on the gain/loss rate again. For weak losses/gains ($\gamma < 0.03\beta$), the entanglement between the cavities 1-2, 2-3, 1-3 is significant, but the strongest entanglement can be observed between subsystems 2 and 3. For strong losses/gain, the entanglement between the cavities 1-2, 2-3 plays the main role, whereas the entanglement between modes 3-4, 2-4, 1-4 is not produced.

In the next analyzed case, for $t = 0$, the third cavity is in the one-photon state and the evolution of the system starts from the state $\hat{\rho}(t=0) = |0010\rangle\langle 0010|$. Figure 3c shows that with increasing parameter γ, all bipartite entanglements become weaker and entanglement between subsystems 1-4 and 2-4 disappears. For small values of γ/β, when the strength of the loss/gain rate increases, the maximal values of all negativities significantly decrease. Whereas, for greater values of γ, the values of negativities describing entanglement between modes 1-2, 2-3, 1-3 practically remain constant. For $\gamma > 0.2\beta$, the strongest entanglement we observe is between two neutral cavities.

In the last case, the system's evolution starts from state $\hat{\rho}(t=0) = |0001\rangle\langle 0001|$, and the excitation initially appears in the active cavity. In Figure 3d, we see that analogously as in the previous case, with increasing γ the maximal values of all negativities decrease. What is interesting is that in such a case, all negativities reach nonzero values. The entanglement between cavities 3 and 4 plays the main role. For subsystems 1-2, 2-3, 1-3, 2-4, the entanglement is weaker, and the weakest correlation we observe is between passive and active cavities 1-4. For small values of γ, the negativity N_{14} significantly decreases; and for $\gamma > 0.2\beta$ reaches values close to zero ($N_{14} < 0.01$).

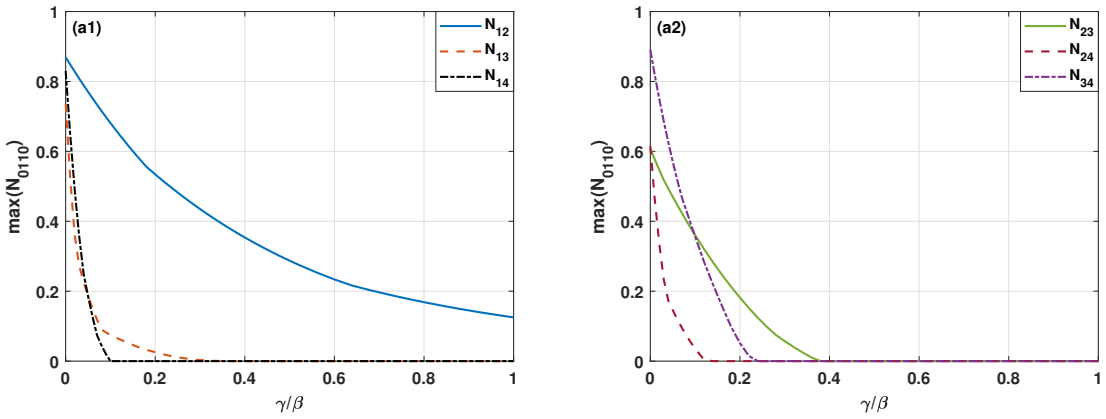

Figure 3. *Cont.*

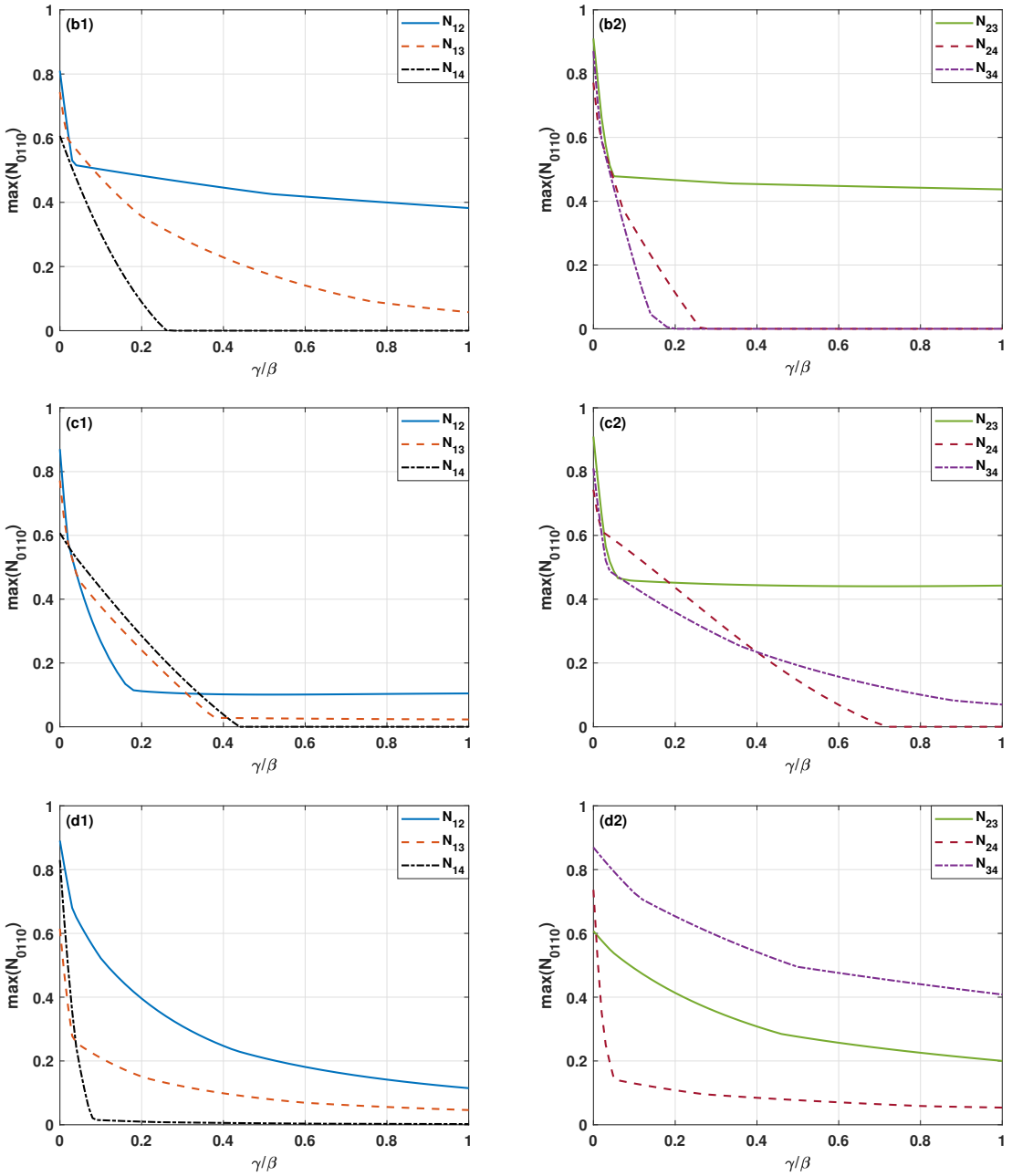

Figure 3. Maximal values of the negativity versus γ/β for $\omega = 2\beta$ and for various initial states: (**a**) $|1000\rangle\langle 1000|$, (**b**) $|0100\rangle\langle 0100|$, (**c**) $|0010\rangle\langle 0010|$, (**d**) $|0001\rangle\langle 0001|$.

4. Conclusions

Obtaining an entanglement quantum state plays a crucial role in the quantum information theory. The entangled states have many possible applications, such as teleportation and dense coding. Quantum correlations, including entanglement, play a significant role in the development of quantum computation and quantum information processing. Therefore, it is important to understand the entanglement nature of quantum systems. In recent years, a lot of papers have been presented on characterizing entanglement in bipartite systems. The entanglement in such systems can be analyzed relatively easily. The quantum correlations in systems consisting of more than two subsystems have not been understood well, so they are extensively studied. Therefore, we were interested in studying the ability of a $\mathcal{PT}$-symmetric system to generate the entangled states, which are especially interesting

from the point of view of quantum information theory. The purpose of this article was to contribute to studies by addressing the entanglement generation.

In this paper, the optical quadrimer system containing four cavities characterized by frequency ω was discussed. The cavities were coupled with each other in such a way that the system formed a chain. Additionally, the first and the last cavity were a subject of losses and gains of energy, respectively, and the rate of losses and gain was balanced.

For such a system, we have found a phase-transition point, and we have shown that when the gain/loss rate is equal or smaller than coupling parameter, all eigenvalues of the system's Hamiltonian are real. In other words, the system is $\mathcal{PT}$-symmetric, contrary to the situation when the gain/loss rate reaches values greater than that of coupling strength and the optical quadrimer is in the broken $\mathcal{PT}$-symmetric phase. For such a case, the system has complex eigenvalue spectra.

We have analyzed four situations corresponding to the four various initial states of the system. We were interested in the possibility of generation of entangled states and the influence of the gain/loss rate strength on the effectiveness of production of such states. We have shown that the degree of entanglement strongly depends on the value of the parameter γ. We have estimated the range of such values for which the strongest bipartite entanglement can be created. For all analyzed cases, when the values of loss/gain rate are small, with increasing γ, the entanglements significantly decrease. For the greater values of loss/gain rate, if the initially active or passive cavity is excited, the strongest entanglement appears between the cavity which, for $t = 0$, is in one-photon state and its nearest neighbor. For the initial time, when one of the neutral cavities is excited, we can observe the strongest entanglement between subsystems 2 and 3.

Funding: The results described in the present work were achieved with the financial support of the ERDF/ESF project "Nanotechnologies for Future" (CZ.02.1.01/0.0/0.0/16_019/0000754) and the program of the Polish Minister of Science and Higher Education under the name "Regional Initiative of Excellence" in 2019–2022, project no. 003/RID/2018/19, funding amount 11 936 596.10 PLN.

Conflicts of Interest: The author declare no conflict of interest. The funders had no role in the design of the study; in the collection, analyses, or interpretation of data; in the writing of the manuscript; or in the decision to publish the results.

References

1. Bender, C.M.; Boettcher, S. Real Spectra in Non-Hermitian Hamiltonians Having $\mathcal{PT}$ Symmetry. *Phys. Rev. Lett.* **1998**, *80*, 5243–5246. [CrossRef]
2. Bender, C.M.; Brody, D.C.; Jones, H.F. Complex Extension of Quantum Mechanics. *Phys. Rev. Lett.* **2002**, *89*, 270401. [CrossRef] [PubMed]
3. Bender, C.M. Making sense of non-Hermitian Hamiltonians. *Rep. Prog. Phys.* **2007**, *70*, 947. [CrossRef]
4. El-Ganainy, R.; Makris, K.G.; Christodoulides, D.N.; Musslimani, Z.H. Theory of coupled optical $\mathcal{PT}$-symmetric structures. *Opt. Lett.* **2007**, *32*, 2632–2634. [CrossRef] [PubMed]
5. Ramezani, H.; Schindler, J.; Ellis, F.M.; Günther, U.; Kottos, T. Bypassing the bandwidth theorem with $\mathcal{PT}$ symmetry. *Phys. Rev. A* **2012**, *85*, 062122. [CrossRef]
6. Miri, M.A.; Regensburger, A.; Peschel, U.; Christodoulides, D.N. Optical mesh lattices with $\mathcal{PT}$ symmetry. *Phys. Rev. A* **2012**, *86*, 023807. [CrossRef]
7. Graefe, E.M.; Jones, H.F. $\mathcal{PT}$-symmetric sinusoidal optical lattices at the symmetry-breaking threshold. *Phys. Rev. A* **2011**, *84*, 013818. [CrossRef]
8. Tchodimou, C.; Djorwe, P.; Nana Engo, S.G. Distant entanglement enhanced in $\mathcal{PT}$-symmetric optomechanics. *Phys. Rev. A* **2017**, *96*, 033856. [CrossRef]
9. Turitsyna, E.G.; Shadrivov, I.V.; Kivshar, Y.S. Guided modes in non-Hermitian optical waveguides. *Phys. Rev. A* **2017**, *96*, 033824. [CrossRef]
10. Zhang, L.L.; Gong, W.J. Transport properties in a non-Hermitian triple-quantum-dot structure. *Phys. Rev. A* **2017**, *95*, 062123. [CrossRef]
11. Mostafazadeh, A. Invisibility and $\mathcal{PT}$ symmetry. *Phys. Rev. A* **2013**, *87*, 012103. [CrossRef]

12. Lü, X.Y.; Jing, H.; Ma, J.Y.; Wu, Y. $\mathcal{PT}$-Symmetry-Breaking Chaos in Optomechanics. *Phys. Rev. Lett.* **2015**, *114*, 253601. [CrossRef] [PubMed]
13. Mostafazadeh, A. Pseudo-Hermiticity versus $\mathcal{PT}$ symmetry: the necessary condition for the reality of the spectrum of a non-Hermitian Hamiltonian. *J. Math. Phys.* **2002**, *43*, 205. [CrossRef]
14. Bender, C.M.; Gianfreda, M.; Özdemir, C.K.; Peng, B.; Yang, L. Twofold transition in $\mathcal{PT}$-symmetric coupled oscillators. *Phys. Rev. A* **2013**, *88*, 062111. [CrossRef]
15. El-Ganainy, R.; Khajavikhan, M.; Ge, L. Exceptional points and lasing self-termination in photonic molecules. *Phys. Rev. A* **2014**, *90*, 013802. [CrossRef]
16. Demange, G.; Graefe, E.M. Signatures of three coalescing eigenfunctions. *J. Phys. A Math. Theor.* **2011**, *45*, 025303. [CrossRef]
17. Heiss, W.D.; Cartarius, H.; Wunner, G.; Main, J. Spectral singularities in $\mathcal{PT}$-symmetric Bose-Einstein condensates. *J. Phys. A Math. Theor.* **2013**. *46*, 275307. [CrossRef]
18. Eleuch, H.; Rotter, I. Clustering of exceptional points and dynamical phase transitions. *Phys. Rev. A* **2016**, *93*, 042116. [CrossRef]
19. Pick, A.; Lin, Z.; Jin, W.; Rodriguez, A.W. Enhanced nonlinear frequency conversion and Purcell enhancement at exceptional points. *Phys. Rev. B* **2017**, *96*, 224303. [CrossRef]
20. Lin, Z.; Pick, A.; Lončar, M.; Rodriguez, A.W. Enhanced Spontaneous Emission at Third-Order Dirac Exceptional Points in Inverse-Designed Photonic Crystals. *Phys. Rev. Lett.* **2016**, *117*, 107402. [CrossRef]
21. Eleuch, H.; Rotter, I. Resonances in open quantum systems. *Phys. Rev. A* **2017**, *95*, 022117. [CrossRef]
22. Zhang, Y.; Zhang, Z.; Yuan, J.; Kang, M.; Chen, J. High-order exceptional points in non-Hermitian Moiré lattices. *Front. Phys.* **2019**, *14*, 53603. [CrossRef]
23. Pick, A.; Zhen, B.; Miller, O.D.; Hsu, C.W.; Hernandez, F.; Rodriguez, A.W.; Soljačić, M.; Johnson, S.G. General theory of spontaneous emission near exceptional points. *Opt. Express* **2017**, *25*, 12325–12348. [CrossRef] [PubMed]
24. Regensburger, A.; Bersch, C.; Miri, M.A.; Onishchukov, G.; Christodoulides, D.; Peschel, U. Parity-time synthetic photonic lattices. *Nature* **2012**, *488*, 167–171. [CrossRef] [PubMed]
25. Peng, B.; Özdemir, C.K.; Rotter, S.; Yilmaz, H.; Liertzer, M.; Monifi, F.; Bender, C.M.; Nori, F.; Yang, L. Loss-induced suppression and revival of lasing. *Science* **2014**, *346*, 328–332. [CrossRef] [PubMed]
26. Zhang, M.; Helmerson, K.; You, L. Entanglement and spin squeezing of Bose-Einstein-condensed atoms. *Phys. Rev. A* **2003**, *68*, 043622. [CrossRef]
27. Vidal, J.; Palacios, G.; Aslangul, C. Entanglement dynamics in the Lipkin-Meshkov-Glick model. *Phys. Rev. A* **2004**, *70*, 062304. [CrossRef]
28. Mohamed, A.; Eleuch, H. Non-classical effects in cavity QED containing a nonlinear optical medium and a quantum well: Entanglement and non-Gaussianity. *Eur. Phys. J. D* **2015**, *69*, 191. [CrossRef]
29. Loss, D.; DiVincenzo, D.P. Quantum computation with quantum dots. *Phys. Rev. A* **1998**, *57*, 120–126. [CrossRef]
30. Miranowicz, A.; Özdemir, Ş.K.; Liu, Y.X.; Koashi, M.; Imoto, N.; Hirayama, Y. Generation of maximum spin entanglement induced by a cavity field in quantum-dot systems. *Phys. Rev. A* **2002**, *65*, 062321. [CrossRef]
31. Cirac, J.I.; Zoller, P. Quantum Computations with Cold Trapped Ions. *Phys. Rev. Lett.* **1995**, *74*, 4091–4094. [CrossRef] [PubMed]
32. Kurpas, M.; Dajka, J.; Zipper, E. Entanglement of qubits via a nonlinear resonator. *J. Phys. Condens. Matter* **2009**, *21*, 235602. [CrossRef] [PubMed]
33. Alexanian, M. Dynamical generation of maximally entangled states in two identical cavities. *Phys. Rev. A* **2011**, *84*, 052302. [CrossRef]
34. Almutairi, K.; Tanaś, R.; Ficek, Z. Generating two-photon entangled states in a driven two-atom system. *Phys. Rev. A* **2011**, *84*, 013831. [CrossRef]
35. Owen, E.T.; Dean, M.C.; Barnes, C.H.W. Generation of entanglement between qubits in a one-dimensional harmonic oscillator. *Phys. Rev. A* **2012**, *85*, 022319. [CrossRef]
36. Brida, G.; Chekhova, M.; Genovese, M.; Krivitsky, L. Generation of different Bell states within the spontaneous parametric down-conversion phase-matching bandwidth. *Phys. Rev. A* **2007**, *76*, 053807. [CrossRef]
37. Coto, R.; Orszag, M.; Eremeev, V. Generation and protection of a maximally entangled state between many modes in an optical network with dissipation. *Phys. Rev. A* **2016**, *93*, 062302. [CrossRef]

38. Ficek, Z.; Tanaś, R. Dark periods and revivals of entanglement in a two-qubit system. *Phys. Rev. A* **2006**, *74*, 024304. [CrossRef]
39. Ficek, Z.; Tanaś, R. Delayed sudden birth of entanglement. *Phys. Rev. A* **2008**, *77*, 054301. [CrossRef]
40. Al-Qasimi, A.; James, D.F.V. Sudden death of entanglement at finite temperature. *Phys. Rev. A* **2008**, *77*, 012117. [CrossRef]
41. López, C.E.; Romero, G.; Lastra, F.; Solano, E.; Retamal, J.C. Sudden Birth versus Sudden Death of Entanglement in Multipartite Systems. *Phys. Rev. Lett.* **2008**, *101*, 080503. [CrossRef] [PubMed]
42. Peres, A. Separability Criterion for Density Matrices. *Phys. Rev. Lett.* **1996**, *77*, 1413–1415. [CrossRef] [PubMed]
43. Horodecki, M.; Horodecki, P.; Horodecki, R. Separability of mixed states: Necessary and sufficient conditions. *Phys. Lett. A* **1996**, *223*, 1–8. [CrossRef]